npj | clean water

www.nature.com/npjcleanwater

ARTICLE OPEN

Check for updates

Biofouling characteristics of reverse osmosis membranes by disinfection-residual-bacteria post seven water disinfection techniques

Hao-Bin Wang[1,2], Yin-Hu Wu[1,2]✉, Wen-Long Wang[3], Li-Wei Luo[1,2], Gen-Qiang Chen[1,2], Zhuo Chen[1,2], Song Xue[1,2], Ao Xu[4], Yu-Qing Xu[1,2], Nozomu Ikuno[5], Kazuki Ishii[5] and Hong-Ying Hu[1,4]

Reverse osmosis (RO) is widely used in wastewater reclamation to alleviate the increasingly global water shortage. However, it has an inconvenient defect of biofouling. Some disinfection processes have been reported to select certain undesirable disinfection-residual bacteria (DRB), leading to severe long-term biofouling potential. To provide constructive guidance on biofouling prevention in RO systems, this study performed a 32-day experiment to parallelly compared the biofouling characteristics of RO membranes of DRB after five mature water disinfection methods (NaClO, NH_2Cl, ClO_2, UV, and O_3) and two recently developed water disinfection methods (K_2FeO_4 and flow-through electrode system). As a result, the DRB biofilm of K_2FeO_4 and O_3 caused a slight normalised flux drop (22.4 ± 2.4% and 23.9 ± 1.7%) of RO membrane compared to the control group (non-disinfected, ~27% normalised flux drop). FES, UV, NaClO and ClO_2 caused aggravated membrane flux drop (29.1 ± 0.3%, 33.3 ± 7.8%, 34.6 ± 6.4%, and 35.5 ± 4.0%, respectively). The biofouling behaviour showed no relationship with bacterial concentration or metabolic activity ($p > 0.05$). The thickness and compactness of the biofilms and the organics/bacterial number ratio in the biofilm, helped explain the difference in the fouling degree between each group. Moreover, microbial community analysis showed that the relative abundance of typical highly EPS-secretory and biofouling-related genera, such as *Pseudomonas*, *Sphingomonas*, *Acinetobacter*, *Methylobacterium*, *Sphingobium*, and *Ralstonia*, were the main reasons for the high EPS secreting ability of the total bacteria, resulting in aggravation of biofouling degree ($p < 0.05$). All types of disinfection except for NaClO and ClO_2 effectively prevented pathogen reproduction in the DRB biofilm.

npj Clean Water (2023)6:24 ; https://doi.org/10.1038/s41545-023-00240-2

INTRODUCTION

Water scarcity is a pressing global challenge[1]. In recent years, the accelerated carbon neutrality process contributed to an increasing installation of renewable energy, which consume more water producing the same electric power[2]. As a consequence, this worldwide action against climate change will worsen the water shortages problem[3]. Meanwhile, lots of countries and regions continue to face water contamination[4]. Water reclamation is a win-win strategy for increasing freshwater supply and shortening the water footprint of human beings[5–7].

Reverse osmosis (RO) is one of the most applicable and stable units for high-quality reclaimed water production in industrial reuse, potable reuse, and groundwater replenishment[8–12]. Many large-scale water reclamation plants have been successively operated[13–15]. However, RO system has an inconvenient defect, that is, the complex and rebellious membrane fouling, which leads to the surge of operating cost[16,17]. Membrane fouling of RO mainly includes scaling, colloidal fouling, organic fouling, and biofouling[18]. Among these, biofouling is the most complicated and noteworthy one one[16,19], although numerous studies have made significant efforts to reduce it[20–23].

Disinfection is a widely applied pretreatment process used to deal with biofouling in RO systems. However, it may lead to undesirable effects[22]. After reducing the number of bacteria in the feed water, the disinfection process exerts a salient selection effect on the bacterial community and the extracellular polymeric substance (EPS) secreting ability of the bacteria[13,22,24–26]. Some unwanted bacteria, that are resistant to disinfection or can adapt to adverse environments, might survive disinfection processes and become disinfection-residual-bacteria (DRB)[27,28]. DRB might possess a higher proportion of bacteria with higher EPS secreting ability, leading to a more severe biofouling of RO membranes, especially in the long-term operation of RO systems[29]. Research in laboratory and full-scale water treatment plants has shown the probability of aggravated biofouling after disinfection[24–26,30]. However, most of these studies are limited to a single type of disinfection process[31,32]. To date, there is still a lack of systematic and broad comparison of the biofouling-control effects of various disinfection methods.

To provide more constructive and reliable guidance on the prevention of RO biofouling, this study compared the DRB characteristics of seven different disinfection methods, including five widely used disinfection methods (NaClO, NH_2Cl, ClO_2, UV, and O_3) and two recently developed disinfection methods (K_2FeO_4 and flow-through electrode system (FES)[33]) via a long-term (32 days) biofilm cultivation experiment on RO membranes. Furthermore, the bacteria and organic matter in the biofilm on the

[1]Environmental Simulation and Pollution Control State Key Joint Laboratory, State Environmental Protection Key Laboratory of Microorganism Application and Risk Control (SMARC), School of Environment, Tsinghua University, 100084 Beijing, PR China. [2]Beijing Laboratory for Environmental Frontier Technologies, 100084 Beijing, PR China. [3]Key Laboratory of Microorganism Application and Risk Control of Shenzhen, Institute of Environment and Ecology, Tsinghua Shenzhen International Graduate School, Tsinghua University, Shenzhen 518055, PR China. [4]Research Institute for Environmental Innovation (Suzhou), Tsinghua, Jiangsu, Suzhou 215163, PR China. [5]Kurita Water Industries Ltd., Nakano-ku, Tokyo 164-0001, Japan. ✉email: wuyinhu@mail.tsinghua.edu.cn

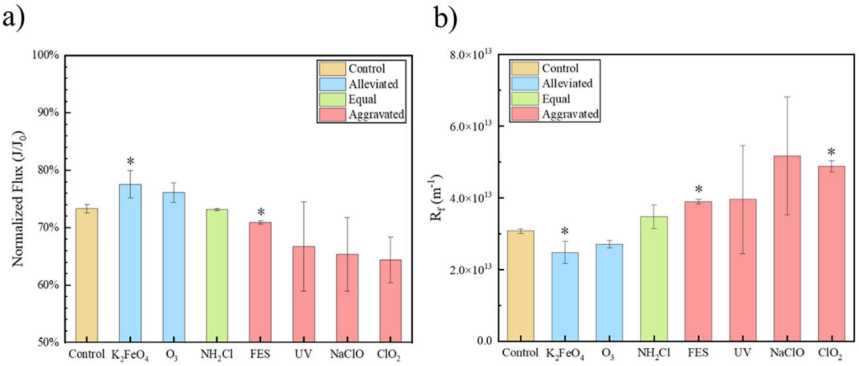

Fig. 1 Fouling degree of RO membranes with DRB biofilm (32 days) after seven different kinds of disinfection treatment. a The normalised flux of fouled membranes and **b** the hydraulic resistance of the biofilms. The experiment was conducted in parallel in three sets. Error bars represent the standard deviation for three independent experiments. The *p* value was generated by *t* test (*$p < 0.05$, **$p < 0.01$).

RO membranes were analysed using heterotrophic plate count (HPC), adenosine triphosphate (ATP), dissolved organic matter (DOM), and fluorescence excitation-emission matrix (EEM) to determine the primary reasons for the differences in biofouling in each group. The microbial community structure of DRB biofilms was analysed using high-throughput sequencing. Based on these results, the correlations among the fouling characteristics of DRB biofilms and bacterial density, organic density, biofilm morphology, and the microbial community of DRB were analysed.

RESULTS

Effects of DRB biofilm on the RO membrane performance

The effects of different water disinfection methods on the RO membrane flux of the DRB biofilms were investigated. Not all disinfection methods can control biofouling. These methods were divided into three groups, according to the normalised flux (Fig. 1a). The first group, classified as "alleviated", included K_2FeO_4 and O_3. Their DRB performed light normalised flux drop (22.4 ± 2.4% and 23.9 ± 1.17%, respectively) compared to the control group (without disinfection pre-treatment), thereby indicating alleviated biofouling potentials. Meanwhile, the DRB of NH_2Cl had a similar biofouling degree as the control group (~27%), and was classified as "equal". Finally, the DRB of the "aggravated" group, which included FES, UV, NaClO, and ClO_2, caused more biofouling of the RO membrane than the control group (29.1 ± 0.3%, 33.3 ± 7.8%, 34.6 ± 6.4%, and 35.5 ± 4.0% flux drop, respectively). The two most frequently used disinfection methods, namely UV and NaClO aggravated the biofouling of RO membranes, matching the results of long-term studies in previous research[24,26]. The initial flux values were shown in Supplementary Table 1.

The hydraulic resistance of the DRB biofilms (*Rm*) is shown in Fig. 1b. The hydraulic resistance of the fouling layer is consistent with the flux drop data ($R^2 = 0.91$, $p < 0.05$). The resistance of the K_2FeO_4-DRB biofilm ($2.48 \times 10^{13}\ m^{-1}$) was the lowest as it had the least impact on the RO membrane flux drop. Also, the resistance of the O_3-DRB biofilm ($2.71 \times 10^{13}\ m^{-1}$) in the "alleviated" group was lower than that of the control group ($3.07 \times 10^{13}\ m^{-1}$). The resistance of the NH_2Cl-DRB biofilm ($3.48 \times 10^{13}\ m^{-1}$) was slightly higher than that of the control group. The DRB biofilm resistance of all the "aggravated" groups was much higher than that of the control group. Among them, the average resistance of NaClO was the highest, at $5.18 \times 10^{13}\ m^{-1}$. However, it had a relatively high within-group error, corresponding to the membrane flux drop shown in Fig. 1a.

Disinfection effect of seven kinds of disinfection methods

Alleviation of biofouling after disinfection might be associated with lower bacterial concentrations in the feed water after disinfection[24]. However, the bacterial concentrations in the feed water could not explain the difference of flux drop in this long-term experiment. Variations in the concentrations of HPC and ATP in the water samples during the disinfection processes were tested (Table 1). The five conventional water disinfection methods achieved a bacterial inactivation rate of 3-log, while K_2FeO_4 and FES exhibited a relatively low inactivation effect (~1-log). Overall, HPC had no monotonous correlation with biofouling potential. The DRB biofilm of K_2FeO_4 caused only a 22% decrease in membrane flux, although the inactivation effect of K_2FeO_4 was the lowest (<1-log). NaClO was the most effective method for bacterial inactivation. However, its DRB aggravated biofouling at an average relative flux drop of ~35%.

Table 1. Disinfection effect measured by HPC and ATP content.

Disinfection methods	HPC (CFU/mL)	Inactivation rate (log)	ATP (ng/mL) (Total)	ATP (ng/mL) (Intracellular)
Control	2.7 ± 0.1*10^5	--	2.99 ± 0.08	2.90 ± 0.08
K_2FeO_4	2.4 ± 0.2*10^4	1.06 ± 0.05	0.65 ± 0.01	0.61 ± 0.00
O_3	1.5 ± 0.5*10^2	3.28 ± 0.14	2.93 ± 0.18	0.11 ± 0.01
NH_2Cl	4.3 ± 2.3*10^1	3.88 ± 0.25	0.24 ± 0.02	0.18 ± 0.02
FES	1.6 ± 0.1*10^4	1.23 ± 0.04	0.61 ± 0.02	0.35 ± 0.00
UV	2.5 ± 0.8*10^2	3.06 ± 0.15	5.11 ± 0.24	4.92 ± 0.23
NaClO	3.0 ± 1.0*10^1	3.98 ± 0.14	4.03 ± 0.12	0.21 ± 0.01
ClO_2	1.5 ± 0.1*10^2	3.27 ± 0.01	0.59 ± 0.02	0.45 ± 0.02

Previous studies have reported that ATP can be an effective indicator for predicting biofouling potentials in the short- or medium-term operation of RO systems (less than 16 days)[18,34]. However, this conclusion is not valid in long-term experiments (Table 1). The intracellular ATP in the control group was 2.90 ng/mL, accounting for 97% of the total ATP. Total and intracellular ATP concentrations increased after UV treatment, partly because of the rapid DNA repair mechanism triggered by UV radiation. No correlation was found between the DRB biofouling potentials (membrane flux drop) and the ATP concentration of DRB (Supplementary Fig. 1a, $p > 0.05$). Evaluation of the water disinfection effect suggested that the amount and the activity of DRB were not the decisive factors of biofouling potential during long-term operation.

Characteristics of the DRB biofilm on RO membranes

To determine the reasons for varying performances of RO membranes fouled by different DRB biofilms, this study dissected the fouled RO membranes and performed a series of tests. The number of bacteria and organics in the DRB biofilms, the

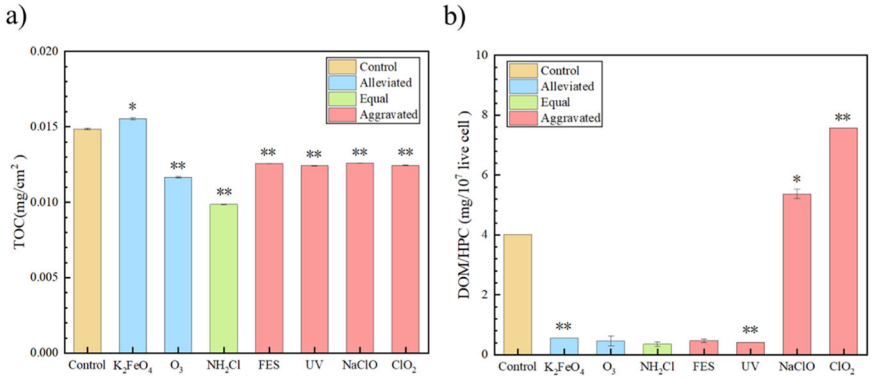

Fig. 2 DOM density in the DRB biofilms (32 days). a DOM content and **b** the ratio of the ratio of DOM to HPC in the biofilms. The experiment was conducted in parallel in three sets. Error bars represent the standard deviation for three independent experiments. The *p* value was generated by *t* test (*$p < 0.05$, **$p < 0.01$).

morphological characteristics of DRB biofilms, and the bacterial community structure were analysed.

The live bacterial density of the DRB biofilm was measured using HPC, as shown in Supplementary Fig. 1b. DRB biofilms of NH_2Cl, FES, and UV possessed the maximum live bacteria density (approximately 10^6 CFU/cm^2). The live bacterial density of NaClO- and ClO_2-DRB biofilms were lower than that of the control group (approximately 10^5 CFU/cm^2), but they led to the worst flux drop in the RO membrane. Hence, the live bacterial density of the DRB biofilm was not a key factor leading to differences in biofouling degrees. This conclusion is consistent with previous studies[26].

Unlike bacterial cells, it has been reported that the extracellular polymeric substances (EPS) on RO membranes have a more direct relationship with flux drop[35,36]. Hence, the total amount of organics in the DRB biofilms was measured by DOM (Fig. 2a), and the different component of DOM was tested using EEM (Supplementary Fig. 2). The amount of DOM did not show a clear correlation with the biofouling degree. The DOM of K_2FeO_4, which was in the "alleviated" group, was much higher than that of the "aggravated" group. Therefore, the total amount of organics did not play a key factor in the degree of DRB biofilm fouling.

Considering that the ratio of EPS to bacteria could affect the biofouling degree[36], this study calculated the ratio of DOM to HPC in the DRB biofilms (Fig. 2b). The DOM/HPC ratio in the control group was approximately 4 mg/10^7 live cells. The DRB biofilm of K_2FeO_4, O_3, NH_2Cl, FES, and UV possessed a relatively lower DOM/HPC ratio, while those of NaClO and ClO_2 (5.4 and 7.6 mg/10^7 live cell, respectively) were significantly higher than the control group ($p < 0.05$). This implied that these two disinfectants could aggravate biofouling of the RO membrane by changing the microbial community and changing the EPS production capacity of the residual bacteria. The DOM/HPC ratio could only partly explained the aggravated biofouling of NaClO and ClO_2 group, it has no statistical association with the flux drop value overall ($R^2 < 0.5$, $p > 0.05$).

The proportions of DOM components among all the groups were similar (Supplementary Fig. 2). Tyrosine/tryptophan amide (Zone I) and protein-containing tyrosine/tryptophan (Zone II) were the dominant components of fluorescent organic matter in each DRB biofilm, indicating that amino acids and proteins were predominant in the DRB biofilms, compared with polysaccharides, fulvic acids, or humid acids.

Compared to the amount of bacteria and organics in the biofilm, the degree of biofouling was more closely correlated with their arrangement and accumulation condition, which resulting in the thickness and consecutiveness of the biofilm on RO membranes[36]. The thickness of the DRB biofilm was tested using z-stack images of the LSCM. The surface image of the DRB biofilm showed that bacteria, proteins, and α-/β-polysaccharides were

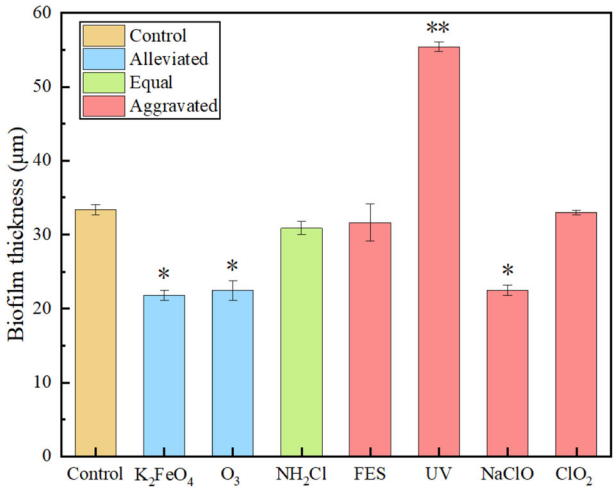

Fig. 3 Thickness of DRB biofilms (32 days). The thickness of biofilms were measured with laser scanning confocal microscope (LSCM). Ten points were randomly taken and averaged. Error bars represent the standard deviation for each independent experiments. The *p* value was generated by *t* test (*$p < 0.05$, **$p < 0.01$).

evenly distributed in the DRB biofilm (Supplementary Fig. 3). The DRB biofilm of K_2FeO_4 was relatively loose in section view, while the others were consecutive (Supplementary Fig. 4). The average thickness of the DRB biofilm was measured via cross-section (Supplementary Fig. 4) and is shown in Fig. 3. As a result, the DRB biofilm of the UV group (55 ± 1 μm) was significantly thicker than that of the control group (33 ± 1 μm) ($p < 0.01$). The DRB biofilm thickness of the "alleviated" group was approximately 22 μm, which was the lowest of all the groups. The biofilm thickness partly illustrated the difference in the biofouling degree, supplemented by the DOM/HPC ratio. The two disinfection methods in the "alleviated" group caused a low DOM/HPC ratio and thinner biofilm on the RO membrane, leading to a marginal flux drop of the fouled membrane. The UV DRB developed a thick biofilm and led to severe biofouling of the RO membrane. This association was not statistical significance ($p > 0.05$, $R^2 < 0.5$). There were also counter examples. For instance, the biofilms of NaClO and ClO_2 were not very thick. However, the high DOM/HPC ratio in the biofilm could narrow the water channels between bacterial cells[36], leading to the highest flux drop in the RO membrane. Therefore, neither the thickness or the density of biomass in the biofilm was the decisive factor. These two factors jointly affected the degree of RO membrane fouling.

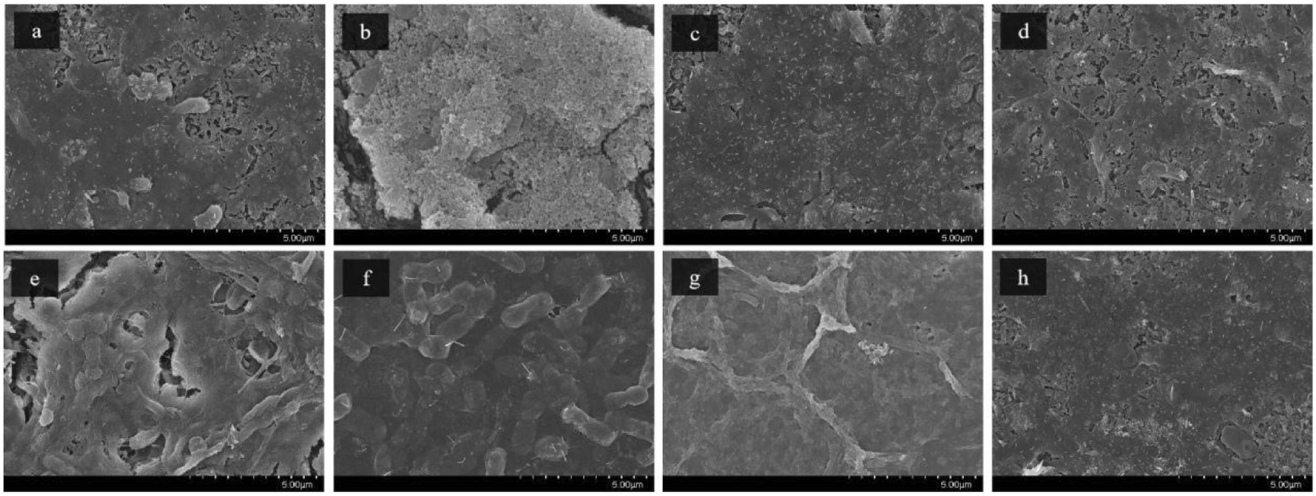

Fig. 4 Scanning electron microscope (SEM) images of DRB biofilms. SEM images of DRB biofilms developed on the surface of RO membranes was taken by field-emission scanning electron microscopy. **a** control group, **b** K_2FeO_4 group, **c** O_3 group, **d** NH_2Cl group, **e** FES group, **f** UV group, **g** NaClO group, and **h** ClO_2 group.

In addition, we also use electron microscopy to observe the morphology of biofilms. The FESEM images of the DRB biofilm are shown in Fig. 4. The DRB biofilm fully covered all the RO membranes. However, the compactness of the biofilms was different. The UV and NaClO-DRB biofilms were compact and continuous, partly illustrating their severe biofouling performance. In contrast, there were gaps between the bacteria and the EPS matrix in the DRB biofilm of the remaining groups. Regular crystals containing Fe were observed in the K_2FeO_4 group (Supplementary Fig. 5), indicating that K_2FeO_4 could cause scaling of the RO membrane.

Microbial community analysis of DRB biofilm on RO membranes

Disinfection processes can exert three levels of change on the bacteria: metabolic change of a single bacteria, shift in the microbial community, and variation of nutrient conditions[27]. Among them, a shift in the microbial community is most likely to affect the biofouling degree during long-term operations[37]. Therefore, we analysed the alpha and beta diversities of the DRB microbial community.

The alpha diversity indices of the observed species as well as the ACE, Chao1, and Shannon indices of bacteria in the DRB biofilm are listed in Supplementary Table 2. The community richness and evenness of the control group were the highest, followed by K_2FeO_4 ("alleviated" group), which has been reported to have minimal impact on the bacterial community[38]. The community evenness of the ClO_2-DRB biofilm ("aggravated" group) was the lowest, indicating a significant selection effect of ClO_2. Overall, community richness and evenness did not show a monotonous correlation with the biofouling behaviour of DRB biofilms.

A Venn diagram of the OTUs that appeared in each group is shown in Supplementary Figure 6. Only 36 OTUs were shared by all the groups. The control group had the highest OTUs, indicating that each water disinfection method had a selection effect. Besides the control group, the number of OTUs in the K_2FeO_4-DRB biofilm was the highest. High numbers of OTUs caused fierce competition among the species, and inhibited biofilm growth and EPS secreting, resulting in the least biofouling of the K_2FeO_4-DRB biofilm. The DRB biofilm with ClO_2 and O_3 disinfection possessed the lowest OTUs, indicating that the two aforementioned oxidising disinfection methods had strong selectivity for the bacteria[39]. However, as their biofouling performance differed, ClO_2 selected more biofilm formation and EPS-secreting species than O_3.

The microbial community structure at the phylum level is shown in Supplementary Fig. 7a, a heat map at the genus level is shown in Supplementary Fig. 7b. The microbial community structure at class and genus levels are shown in Supplementary Fig. 8. α-Proteobacteria and γ-Proteobacteria were the dominant classes in all the DRB biofilms. Actinobacteria and Bacteroidetes were the second and third most abundant phyla, respectively. The top three phyla accounted for 90% of all bacteria.

Previously reported biofouling-related genera had significantly higher relative abundances in the "aggravated" group, namely, ClO_2, NaClO, UV, and FES. For instance, *Methylobacterium*, which is a typical disinfection-resistant and biofouling-related bacteria genus[24,36], was dominant in the DRB biofilm of FES and ClO_2 with a relative abundance of $54.8 \pm 2.3\%$ and $28.6 \pm 1.7\%$, respectively. *Sphingobium*, a highly secretory genus[26,40], was found to dominate the DRB biofilm under UV ($30.0 \pm 0.8\%$). In addition, the relative abundance of *Pseudomonas* was significantly higher in the NaClO-DRB biofilm than in the other groups ($45.9 \pm 1.8\%$) ($p < 0.05$). *Pseudomonas*, which is a typical DRB of chlorine[27] causes biofouling of RO membranes[24,41–43]. In contrast, the relative abundance of these genera was significantly lower in the K_2FeO_4-and O_3-DRB biofilms (<10%) ($p < 0.05$). Thus, the relative abundance of highly secretory or biofouling-related genera plays a decisive role in the biofouling potential of DRB during long-term operation.

A community structure similarity analysis was performed using the PCA algorithm (Fig. 5). The community structures of all the disinfection groups were highly different from those of the control group. The bacterial community structures of UV-, O_3-, NH_2Cl-, NaClO-, and K_2FeO_4-DRB biofilms were similar, whereas the community structures of ClO_2 and FES DRB biofilms were similar. This may be the cause of the inability of these two disinfectants to control the highly secretory genus *Methylobacterium*.

Apart from biofouling of RO membranes, the DRB biofilm can act as a shelter for pathogenic bacteria, leading to health risks of RO concentrate[44]. Thus, the cumulative relative abundance of pathogens and opportunistic pathogens in the DRB biofilm was analysed and shown in Supplementary Fig. 9. The relative abundance of pathogenic bacteria in the DRB biofilm increased significantly after disinfection with NaClO and ClO_2 ($p < 0.01$), indicating that these two chlorine-containing oxidative disinfectants selected (opportunistic) pathogens. K_2FeO_4, FES, and NH_2Cl

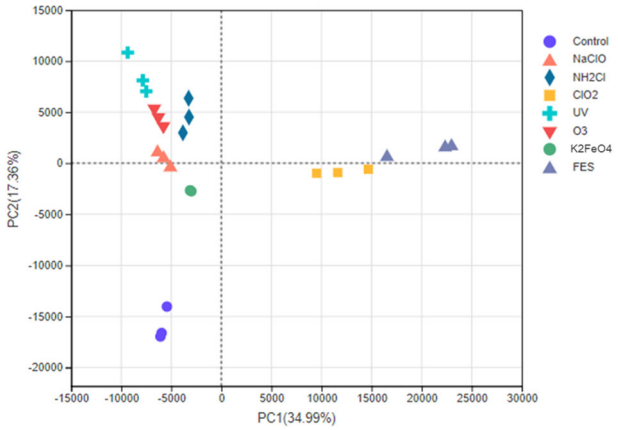

Fig. 5 Principal component analysis (PCA) of microbial communities. Microbial communities of DRB biofilms were displayed in a two-dimensional chart by PCA algorithm. $n = 3$ for all the experiment groups and the control group.

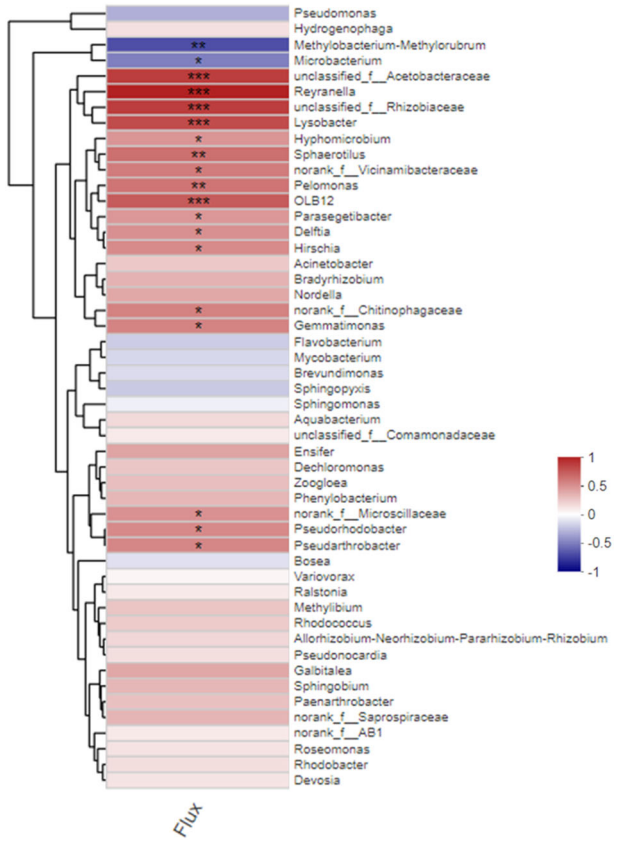

Fig. 6 The correlation between the normalised flux of and relative abundance of the top 50 genera. Heat maps shows the correlation coefficient between normalised flux and relative abundance of the top 50 genera. The p value was generated by Pearson correlation analysis (*$p < 0.1$, **$p < 0.05$, ***$p < 0.01$). The colour indicated the correlation coefficient (dark red: 1, dark blue: −1).

partially reduced the relative abundance of (opportunistic) pathogens. Furthermore, their abundance in DRB biofilms of O_3 and UV were the lowest, demonstrating that they controlled the spread of (opportunistic) pathogens in biofilms. Total read count of OTUs belonging to pathogens and opportunistic pathogens were listed in Supplementary Table 3, showing similar results to the relative abundance. The rising abundance of pathogens and opportunistic pathogens in the NaClO and ClO_2 raised the concerns about potential health risks after these water disinfection processes. As the salient health concern and high social impact, further studies shall pay attention to the absolute abundance of potential pathogens, such as the cell number, gene copy number, and DNA concentration in each type of DRB biofilms.

Correlation between microbial community structure and RO membrane flux

To identify the key genera in the microbial community of DRB affecting the RO membrane flux, correlation coefficients between the normalised flux and relative abundance of the top 50 genera in all the experimental groups and the control group are shown in Fig. 6. The relative abundance of *Methylobacterium* (a typical disinfection-resistance and biofouling-related genus[24,36]) was negatively correlated with the normalised flux of the fouled RO membrane ($p < 0.05$). The relative abundances of two kinds of high EPS-secreting bacteria, *Microbacterium* and *Pseudomonas*, were also negatively correlated with the normalised flux. These two genera consist of typical chlorine-resistant and highly secretory bacteria. Hence, *Methylobacterium*, *Microbacterium*, and *Pseudomonas* deserve special attention as they play an essential role in the aggravated biofouling potential after disinfection.

Additionally, we calculated the accumulative relative abundance of typical highly secretory or biofouling-related genera reported in the literature, including *Pseudomonas*, *Sphingomonas*, *Acinetobacter*, *Methylobacterium*, *Sphingobium*, and *Ralstonia*[24–26,40,41,45] (Fig. 7). The cumulative relative abundance of these bacteria in the "aggravated" group, namely the FES, UV-, NaClO-, and ClO_2- DRB biofilms was significantly higher than that in the control group (~5%). Remarkably, the highly secretory bacteria accounted for over half of the total bacteria in the DRB biofilms of FES and NaClO, that is 56.4% and 53.0%, respectively.

In contrast, the DRB biofilm of the "alleviated" group possessed a similar proportion of highly secretory bacteria as that of the control group. The decrease in bacterial numbers after disinfection could explain biofouling alleviation. Therefore, variation in the relative abundance of typical highly secretory and biofouling-related genera was the main reason for the change in biofouling potentials after different disinfection processes.

DISCUSSION

In the long-term experiment (32 days), DRB biofilms of seven types of water disinfection technics caused various flux dropped, which showed no significant correlation with the bacterial concentration in the feed water. DRB biofilm in the K_2FeO_4 and O_3 group resulted in alleviated biofouling compared to the control group. Biofouling degree of the NH_2Cl-DRB biofilm was similar to that of the control group, whereas the other four types of disinfection aggravated membrane biofouling. Furthermore, as ferrate introduced iron flocs and aggravated inorganic scaling in RO systems, O_3 was recommended as a practical approach to prevent biofouling in RO systems.

The hydraulic resistance of the fouling layer was consistent with the flux drop value. The amount and metabolic of bacteria and the amount of organic matter in the biofilm did not explain the difference in fouling. Morphological analysis combined with the DOM/HPC ratio explained the difference in the fouling behaviour of the DRB biofilms. A high DOM/HPC ratio along with denser and thicker DRB biofilms led to severe biofouling.

Community analysis revealed that the selection effect of disinfection on typical highly secretory and biofouling-related genera was the primary reason leading to the ascending of the EPS secreting capacity of the total bacteria and resulting the high DOM/HPC ratio in the biofilm. The increased relative abundance of these typical bacteria was the radical mechanism for biofouling

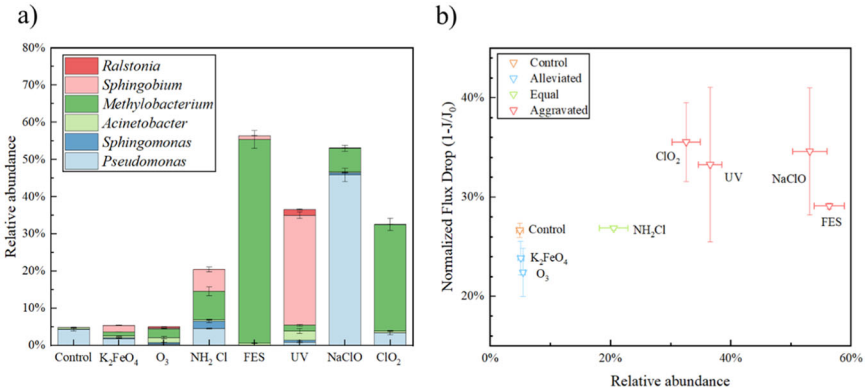

Fig. 7 The relationship between normalised flux drop and relative abundance of typical highly secretory. a Accumulative relative abundance of typical highly secretory or biofouling-related genera reported by previous research and **b** its correlation with normalised flux drop of RO membranes. The correlation coefficient and *p* value were generated by Pearson correlation analysis ($R^2 = 0.64$, $p < 0.05$).

aggravation. Typical genera included *Pseudomonas*, *Sphingomonas*, *Acinetobacter*, *Methylobacterium*, *Sphingobium*, and *Ralstonia*.

All disinfection techniques except for NaClO and ClO_2 effectively reduced the proportion of (opportunistic) pathogens in the DRB biofilm. The absolutely abundance of (opportunistic) pathogens need to be focused in further studies.

METHODS

Water samples

Reclaimed water was sampled from a large-scale water reclaimed plant in Beijing, China. A schematic of the advanced treatment process is shown in Supplementary Fig. 10. The effluent from the denitrification filter was chosen as the sample because subsequent treatment units had a bacterial removal effect[46]. The reclaimed water samples were transported to the laboratory within 1 h, then filtered by filter papers to remove particles, and kept at 4 °C before disinfection. Water quality parameters of the sampled water were measured as soon as they arrived at the laboratory, and are listed in Supplementary Table 4.

Disinfection and biofilm culture

Five commonly used water disinfection methods, including NaClO, NH_2Cl, ClO_2, UV, and O_3, and two recently developed water disinfection technologies, namely K_2FeO_4 and a flow-through electrode system (FES), were compared in this study. The steps followed in the experiment are shown in Supplementary Fig. 11. Briefly, water samples were filtered using filter paper (medium speed, Newstar, Hangzhou, China) to remove large flocs before disinfection. Seven types of disinfection processes were conducted following the technical parameters described in preliminary experiments (Table 2) to achieve similar bacterial log removal, except for two recently developed water disinfection methods as they could not achieve a high disinfection effect in actual wastewater. Square-wave alternating pulse current FES devices were set up based on a previous study[33]. The voltage amplitude and hydraulic retention time were set at 4 V and 27.7 s, respectively, to achieve the best disinfection performance of the system. UV irradiation was performed using a laboratory-scale collimated light-beam apparatus[26,47]. Other oxidising disinfection processes were performed in sterilised glass bottles at 25 °C and 150 rpm. The reaction was quenched with $Na_2S_2O_3$ solution (10 mg/L, 10 min) to avoid oxidative damage to the RO membrane[36,48,49].

Aromatic polyamide composite LP100 RO membrane (Vorton, China) was cut into round coupons (d = 32 mm, S = 804 mm^2), and the pretreatment procedure was conducted based on a previous study[50]. For biofilm culturing, the membrane coupon was soaked in 18 mL of disinfected water or control samples in a 5 cm sterilised round plastic Petri dish at 25 °C. Water samples were refreshed daily. After 32 days of culture, the membrane was gently rinsed twice with phosphate buffer saline (PBS) to remove suspending bacteria for sequencing analysis. The experiments were conducted in triplicates for each group.

Table 2. Dosage of each disinfection method.

Disinfection method	Free chlorine	Chloramine	Chlorine dioxide	UV
Dosage	5 mg/L 30 min	5 mg/L 30 min	1 mg/L 30 min	30 mJ/cm^2
Disinfection method	Ozone	Ferret	FES	
Dosage	3 mg/L 10 min	5 mg/L 10 min	E = 4 V, T = 27.7 s	

Evaluation of the water disinfection effect

The water disinfection effect was evaluated based on the concentration of culturable bacteria; ATP was tested before the biofilm culture experiments with triplicate experiments immediately after the disinfection processes were completed. Culturable bacteria were measured by HPC via colony-forming unit (CFU) counting[46]. ATP was tested using luminescence analysis. For total ATP measurement, 100 µL of the bacterial suspension and 100 µL of CellTiter-Glo Luminescent Cell Viability Assay (Promega, USA) were mixed in 96-well plates. After incubation at 25 °C and at 150 rpm in the dark for 1 min, luminescence intensity was measured using a microplate reader (SpectraMax M5, Molecular Devices, USA). For the extracellular ATP test, water samples were filtered through a 0.1 µm membrane (Millipore) to remove bacteria; the subsequent steps were the same as those for total ATP. Intracellular ATP concentration was calculated by subtracting the extracellular ATP concentration from the total ATP concentration.

RO cross-flow unit and membrane performance tests

A laboratory-scale cross-flow RO system was used to evaluate the performance of RO membranes before and after biofilm growth[35]. Briefly, the membrane compaction phase was performed with a 30 min rinse of ultra-pure water at 1.2 MPa until the permeate flux was stable. The flow rate of the influent was set at 1.0 mL/min via a constant flow pump (NPL-100). The crossflow velocity was set as 6.23 cm/s, which was relatively low value within the actual operating range, to protect the biofilm from cracking[51–54]. The feed water was then switched to a 500 mg/L NaCl solution (conductivity of approximately 1000 µs/cm). The permeate flux

was recorded after reaching a constant value. The normalised flux was calculated by dividing the flux of the fouled membrane by the clean membrane before biofilm growth.

The resistance of the biofilm on the RO membrane was calculated, as follows:

$$R_b = R_T - R_m - R_P = \frac{\Delta P}{\sigma J} - R_m - R_P \quad (1)$$

Where, ΔP is the transmembrane pressure, σ is the kinetic viscosity of water, and J is the flux. The resistance of the biofilm R_b is calculated by subtracting the resistance of the virgin membrane R_m and the resistance of the concentration polarisation R_p from the resistance of the fouled membrane R_T.

Biofilm analysis

Microbial amount and activity were determined using HPC and ATP concentrations. A piece of 10 mm × 10 mm fouled membrane was cut off and vortexed in 0.5 mL normal saline for 30 s. HPC and ATP concentrations were tested using the same procedure, as described in Section "Evaluation of the water disinfection effect".

DOM and EEM were applied to reflect the characteristics of organic matter in DRB biofilms[55]. Briefly, a piece of 10 mm × 10 mm fouled membrane was cut and shaken in 5 mL NaOH solution (pH 12) for 24 h at 25 °C and 150 rpm. Then, HCl solution (pH 2) was added to adjust the pH of the solution to 7.0 ± 0.2. After neutralisation, the volume of the solution was adjusted to 15 mL by adding ultrapure water. The solution was filtered through a 0.45-μm nylon membrane (Whatman, England) before total organic carbon (TOC) measurement on a TOC-5000A analyser. EEM spectra were recorded using a fluorescence spectrophotometre (F-7100, Hitachi, Japan). The EEM spectrum was divided into six zones for integration. The types of fluorescent substances in each zone are shown in Supplementary Table 5[26,56].

A laser scanning confocal microscope (LSCM, LSM710META, Zeiss, Germany) was used to measure the thickness of the biofilm on the RO membrane. A 5 × 10 mm membrane with the DRB biofilm of each sample was cut for LSCM observation. The staining groups of the fluorescent dyes and their targets are listed in Supplementary Table 6. The thickness of biofilm was measured via the section view photos. Ten points were randomly taken and averaged.

The surface morphology of the DRB biofilm was examined using field-emission scanning electron microscopy (FESEM, SU8220, Hitachi, Japan) and the accelerating voltage was set to 5 kV. A piece of 5 × 5 mm membrane coupon was cut for observation.

Three pieces of 40 mm^2 membrane coupons were cut for microbial community analysis. Microbial community analysis was conducted as previously described[24]. Briefly, DNA was extracted using the E.Z.N.A.® soil DNA Kit (Omega Bio-Tek, Norcross, GA, U.S.). Furthermore, bacterial specific primer 338F (5′-ACTCCTACGGGAGGCAGCAG-3′) and 806R (5′-GGACTACHVGGGTWTCTAAT-3′) were used as primer pairs for the amplification of hypervariable region V3-V4 of the bacterial 16S rRNA gene. Sequencing was performed using an Illumina MiSeq PE300 platform. The raw 16S rRNA gene data were demultiplexed, quality-filtered by Fastp version 0.20.0. All analysed sequences were submitted to the NCBI SRA database under accession number PRJNA803872. Data analysis and figure drawing was accomplished with the Bioinformatics Cloud platform of Majorbio (Shanghai, China). Pathogen identification was based on the Virulence Factor Database (VFDB) from the Institute of Pathogen Biology, CAMS & PUMC[57].

Reporting summary

Further information on research design is available in the Nature Research Reporting Summary linked to this article.

DATA AVAILABILITY

DNA sequences are available at the NCBI Sequence Read Archive, accession number: PRJNA803872.

Received: 30 June 2022; Accepted: 1 March 2023;
Published online: 21 March 2023

REFERENCES

1. Gleick, P. H. & Cooley, H. Freshwater scarcity. *Annu. Rev. Environ. Resour.* **46**, 319–348 (2021).
2. Ding, N., Liu, J., Yang, J. & Lu, B. Water footprints of energy sources in China: exploring options to improve water efficiency. *J. Clean. Prod.* **174**, 1021–1031 (2018).
3. Qin, Y. Global competing water uses for food and energy. *Environ. Res. Lett.* **16**, https://doi.org/10.1088/1748-9326/ac06fa (2021).
4. Xu, A. et al. Towards the new era of wastewater treatment of China: development history, current status, and future directions. *Water Cycle* **1**, 80–87 (2020).
5. Wencki, K. et al. Approaches for the evaluation of future-oriented technologies and concepts in the field of water reuse and desalination. *J. Water Reuse Desalination* **10**, 269–283 (2020).
6. Takeuchi, H. & Tanaka, H. Water reuse and recycling in Japan — History, current situation, and future perspectives. *Water Cycle* **1**, 1–12 (2020).
7. Wang, X. C. Safe water reuse through a quasi-natural water cycle. *J. Water Reuse Desalination* **12**, 366–372 (2022).
8. Tseng, S. F., Lo, C. M. & Hung, C. H. Evaluation on the benefit of practically operating reverse osmosis system in the factory: taking the recycle of KI solution and water of the screen polarizing plate as an example. *Water Reuse* **11**, 329–346 (2021).
9. Page, D. et al. Progress in the development of risk-based guidelines to support managed aquifer recharge for agriculture in Chile. *Water Cycle* **1**, 136–145 (2020).
10. Farhat, N. M. et al. Application of monochloramine for wastewater reuse: Effect on biostability during transport and biofouling in RO membranes. *J. Membr. Sci.* **551**, 243–253 (2018).
11. Tong, X. et al. Fouling properties of reverse osmosis membranes along the feed channel in an industrial-scale system for wastewater reclamation. *Sci. Total Environ.* **713**, 136673 (2020).
12. Sahu, P. A comprehensive review of saline effluent disposal and treatment: conventional practices, emerging technologies, and future potential. *Water Reuse* **11**, 33–65 (2021).
13. Luo, L. W. et al. Aggravated biofouling caused by chlorine disinfection in a pilot-scale reverse osmosis treatment system of municipal wastewater. *Water Reuse* **11**, 201–211 (2021).
14. Bai, Y. et al. Long-term performance and economic evaluation of full-scale MF and RO process – A case study of the changi NEWater Project Phase 2 in Singapore. *Water Cycle* **1**, 128–135 (2020).
15. Yu, T. et al. Microcoagulation improved the performance of the UF-RO system treating the effluent from a coastal municipal wastewater treatment plant: a pilot-scale study. *Water Reuse* **11**, 177–188 (2021).
16. Qasim, M., Badrelzaman, M., Darwish, N. N., Darwish, N. A. & Hilal, N. Reverse osmosis desalination: a state-of-the-art review. *Desalination* **459**, 59–104 (2019).
17. Yu, T. et al. Effects of chlorine disinfection on RO membrane biofouling at low feed water temperature for wastewater reclamation. *J. Water Reuse Desalination* **12**, 438–450 (2022).
18. Sim, L. N. et al. A review of fouling indices and monitoring techniques for reverse osmosis. *Desalination* **434**, 169–188 (2018).
19. Komlenic, R. Rethinking the causes of membrane biofouling. *Filtration Sep.* **47**, 26–28 (2010).
20. Jahan Sajib, M. S. et al. Atomistic simulations of biofouling and molecular transfer of a cross-linked aromatic polyamide membrane for desalination. *Langmuir* **36**, 7658–7668 (2020).
21. Weinrich, L., LeChevallier, M. & Haas, C. N. Contribution of assimilable organic carbon to biological fouling in seawater reverse osmosis membrane treatment. *Water Res.* **101**, 203–213 (2016).
22. Al-Abri, M. et al. Chlorination disadvantages and alternative routes for biofouling control in reverse osmosis desalination. *NPJ Clean. Water* **2**, 2 (2019).
23. Abushaban, A. et al. Biofouling potential indicators to assess pretreatment and mitigate biofouling in SWRO membranes: a short review. *Desalination* **527**, 115543 (2022).
24. Wang, Y.-H. et al. Chlorine disinfection significantly aggravated the biofouling of reverse osmosis membrane used for municipal wastewater reclamation. *Water Res.* **154**, 246–257 (2019).
25. Khan, M. T., Hong, P.-Y., Nada, N. & Croue, J. P. Does chlorination of seawater reverse osmosis membranes control biofouling? *Water Res.* **78**, 84–97 (2015).

26. Wu, Y.-H. et al. Effect of ultraviolet disinfection on the fouling of reverse osmosis membranes for municipal wastewater reclamation. *Water Res.* **195**, 116995 (2021).
27. Wang, H.-B. et al. Risks, characteristics, and control strategies of disinfection-residual-bacteria (DRB) from the perspective of microbial community structure. *Water Res.* **204**, 117606 (2021).
28. Nordholt, N., Kanaris, O., Schmidt, S. B. I. & Schreiber, F. Persistence against benzalkonium chloride promotes rapid evolution of tolerance during periodic disinfection. *Nat. Commun.* **12**, 6792 (2021).
29. Wang, Y.-H. et al. Metagenomics analysis of the key functional genes related to biofouling aggravation of reverse osmosis membranes after chlorine disinfection. *J. Hazard. Mater.* **410**, 124602 (2021).
30. Luo, L.-W. et al. Aggravated biofouling caused by chlorine disinfection in a pilot-scale reverse osmosis treatment system of municipal wastewater. *J. Water Reuse Desalination* **11**, 201–211 (2021).
31. Zhao, X. et al. Ozonation as an efficient pretreatment method to alleviate reverse osmosis membrane fouling caused by complexes of humic acid and calcium ion. *Front. Environ. Sci. Eng.* **13**, 55, https://doi.org/10.1007/s11783-019-1139-y (2019).
32. Li, G.-Q. et al. Characteristics and mechanism of persulfate activated by natural siderite for water disinfection. *J. Water Reuse Desalination* **12**, 319–331 (2022).
33. Ni, X.-Y. et al. Enhancing disinfection performance of the carbon fiber-based flow-through electrode system (FES) by alternating pulse current (APC) with low-frequency square wave. *Chem. Eng. J.* **410**, 128399 (2021).
34. Weinrich, L., Haas, C. N. & LeChevallier, M. W. Recent advances in measuring and modeling reverse osmosis membrane fouling in seawater desalination: a review. *J. Water Reuse Desalination* **3**, 85–101 (2013).
35. Chen, G.-Q. et al. Enhanced extracellular polymeric substances production and aggravated membrane fouling potential caused by different disinfection treatment. *J. Membr. Sci.* **642**, 120007 (2022).
36. Luo, L.-W. et al. Chlorine-resistant bacteria (CRB) in the reverse osmosis system for wastewater reclamation: isolation, identification and membrane fouling mechanisms. *Water Res.* **209**, 117966 (2021).
37. Podar, M. et al. Microbial diversity analysis of two full-scale seawater desalination treatment trains provides insights into detrimental biofilm formation. *J. Membr. Sci. Lett.* **1**, 100001 (2021).
38. Li, C. et al. Bacterial community structure and microorganism inactivation following water treatment with ferrate(VI) or chlorine. *Environ. Chem. Lett.* **15**, 525–530 (2017).
39. Proctor, C. R. & Hammes, F. Drinking water microbiology—from measurement to management. *Curr. Opin. Biotechnol.* **33**, 87–94 (2015).
40. Zhang, Y. et al. Extracellular polymeric substances enhanced mass transfer of polycyclic aromatic hydrocarbons in the two-liquid-phase system for biodegradation. *Appl. Microbiol. Biotechnol.* **90**, 1063–1071 (2011).
41. Freitas, F., Alves, V. D. & Reis, M. A. M. Advances in bacterial exopolysaccharides: from production to biotechnological applications. *Trends Biotechnol.* **29**, 388–398 (2011).
42. Wei, L. et al. Prevalence, virulence, antimicrobial resistance, and molecular characterization of pseudomonas aeruginosa isolates from drinking water in China. *Front. Microbiol.* **11**, 2984 (2020).
43. Luo, L.-W. et al. Evaluating method and potential risks of chlorine-resistant bacteria (CRB): a review. *Water Res.* **188**, 116474 (2021).
44. Flemming, H.-C. et al. Biofilms: an emergent form of bacterial life. *Nat. Rev. Microbiol.* **14**, 563–575 (2016).
45. Jung, J. & Park, W. Acinetobacter species as model microorganisms in environmental microbiology: current state and perspectives. *Appl. Microbiol. Biotechnol.* **99**, 2533–2548 (2015).
46. Cui, Q. et al. Bacterial removal performance and community changes during advanced treatment process: a case study at a full-scale water reclamation plant. *Sci. Total Environ.* **705**, 8 (2020).
47. Pullerits, K. et al. Impact of UV irradiation at full scale on bacterial communities in drinking water. *NPJ Clean. Water* **3**, 10 (2020).
48. Ding, W. Q. et al. Ozone disinfection of chlorine-resistant bacteria in drinking water. *Water Res.* **160**, 339–349 (2019).
49. Mao, Y. et al. Comparison of the disinfection efficacy between ferrate(VI) and chlorine in secondary effluent. *Sci. Total Environ.* **848**, 157712 (2022).
50. Tong, X. et al. Simulating and predicting the flux change of reverse osmosis membranes over time during wastewater reclamation caused by organic fouling. *Environ. Int.* **140**, 105744 (2020).
51. Suwarno, S. R. et al. Biofouling in reverse osmosis processes: The roles of flux, crossflow velocity and concentration polarization in biofilm development. *J. Membr. Sci.* **467**, 116–125 (2014).
52. Chong, T. H., Wong, F. S. & Fane, A. G. Implications of critical flux and cake enhanced osmotic pressure (CEOP) on colloidal fouling in reverse osmosis: Experimental observations. *J. Membr. Sci.* **314**, 101–111 (2008).
53. Subramani, A. & Hoek, E. M. V. Direct observation of initial microbial deposition onto reverse osmosis and nanofiltration membranes. *J. Membr. Sci.* **319**, 111–125 (2008).
54. Dreszer, C., Flemming, H. C., Zwijnenburg, A., Kruithof, J. C. & Vrouwenvelder, J. S. Impact of biofilm accumulation on transmembrane and feed channel pressure drop: eeffects of crossflow velocity, feed spacer and biodegradable nutrient. *Water Res.* **50**, 200–211 (2014).
55. Mao, Y. et al. Characterization of bacterial fluorescence: insight into rapid detection of bacteria in water. *Water Reuse* **11**, 621–631 (2021).
56. Wang, Z.-P. & Zhang, T. Characterization of soluble microbial products (SMP) under stressful conditions. *Water Res.* **44**, 5499–5509 (2010).
57. Chen, L., Zheng, D., Liu, B., Yang, J. & Jin, Q. VFDB 2016: hierarchical and refined dataset for big data analysis—10 years on. *Nucleic Acids Res.* **44**, D694–D697 (2016).

ACKNOWLEDGEMENTS

This study was supported by the National Key R&D Program of China (No. 2020YFC1806302), the Major Program of National Natural Science Foundation of China (No. 52293440, No. 52293442) and the Science Fund for Creative Research Groups (No. 52221004).

AUTHOR CONTRIBUTIONS

H.-B.W.: Conceptualisation, Methodology, Original draft preparation. Y.-H.W.: Writing-Reviewing and Editing, Project administration, Funding acquisition, Supervision. W.-L.W.: Writing- Reviewing and Editing. L.-W.L.: Conceptualisation. G.-Q.C.: Conceptualisation. Z.C.: Writing- Reviewing and Editing Writing. S.X.: Formal analysis. A.X.: Writing- Reviewing. Y.-Q.X.: Investigation. N.I.: Writing- Reviewing and Resource. K.I.: Resource. H.-Y.H.: Project administration, Supervision.

COMPETING INTERESTS

The authors declare no competing interests.

ADDITIONAL INFORMATION

Supplementary information The online version contains supplementary material available at https://doi.org/10.1038/s41545-023-00240-2.

Correspondence and requests for materials should be addressed to Yin-Hu Wu.

Reprints and permission information is available at http://www.nature.com/reprints

Publisher's note Springer Nature remains neutral with regard to jurisdictional claims in published maps and institutional affiliations.